ELSEVIER

Journal of Alloys and Compounds 437 (2007) 58–63

Journal of ALLOYS AND COMPOUNDS

www.elsevier.com/locate/jallcom

Subsolidus phase relationships of the $BaO–R_2O_3–CuO_z$ (R = Tm and Yb) systems under carbonate-free conditions at $p_{O_2} = 100$ Pa, and $T = 750$ °C and 810 °C

W. Wong-Ng *, Z. Yang, L.P. Cook

Ceramics Division, Materials Science and Engineering Laboratory, National Institute of Standards and Technology, Gaithersburg, MD 20899, USA

Received 13 June 2006; received in revised form 18 July 2006; accepted 19 July 2006
Available online 6 September 2006

Abstract

For applications of phase equilibria to coated conductor processing, phase diagrams constructed under carbonate-free conditions should be employed. Using special apparatus and a procedure for preparing carbonate-free precursors based on BaO, phase diagrams of the $BaO–Tm_2O_3–CuO_z$ and $BaO–Yb_2O_3–CuO_z$ systems were determined at 100 Pa (0.1% O_2 by volume, 750 °C and 810 °C). The $BaO–Yb_2O_3–CuO_z$ system exhibits different features as compared to the Tm-analog. For example, the Yb-system does not contain the $Ba_4RCu_3O_{8.5+z}$ phase. The absence of this phase affects the tie-line relations in the BaO-rich region of the phase diagram of the Yb-system. Furthermore, while the diagrams with relatively large R (i.e., R = Nd, Sm, Eu, Gd, Dy, Er) do not contain a tie-line between $BaCuO_{2+z}$ and BaR_2CuO_5, this tie-line was found in the Yb-diagram, which has a much smaller R. In general, both the diagrams of the $BaO–Tm_2O_3–CuO_z$ and of the $BaO–Yb_2O_3–CuO_z$ systems prepared under carbonate-free conditions are different from those obtained using $BaCO_3$-derived starting materials.
Published by Elsevier B.V.

Keywords: High-T_c superconductors; Solid-state reactions; Phase diagrams; X-ray diffraction

1. Introduction

Since the discovery of the high temperature superconductor oxides [1], considerable technological progress has been achieved in wire and tape development. Intensive research has led to the powder-in-tube (PIT) process for fabrication of Bi–Pb–Sr–Ca–Cu–O (BSCCO) tapes [2–6]. More recently, second-generation high-T_c superconductor (HTS) tapes (also called HTS coated conductors) deposited on flexible coated-conductors have received much attention [7–11]. Second-generation superconductors are based on $Ba_2YCu_3O_{6+z}$ and $Ba_2RCu_3O_{6+z}$ materials (R = lanthanide-substituted variants) [12–15]. The $Ba_2YCu_3O_{6+z}$ and $Ba_2RCu_3O_{6+z}$ materials are relatively more isotropic when compared with BSCCO-based superconductors, and can retain current-carrying ability at liquid nitrogen temperature under high magnetic fields. As a result, HTS coated-conductor have great commercial potential for electric utility and high magnetic field applications. The efforts of the Superconductivity Partnership Initiative of the US Department of Energy have led to a substantial number of prototype applications [16].

Two HTS coated-conductor processes are furthest along in their technological development: the rolling-assisted biaxially textured substrate process (RABiTS) [7–9], and the ion beam-assisted deposition process (IBAD) [10,11]. Phase diagrams provide important data for both processes. Previously, we have reported phase diagram studies of the $BaO–R_2O_3–CuO_z$ systems (R = Nd [17], Sm [18], Y [19], Er, Gd [20], Dy, Ho and Eu [21]) under carbonate-free conditions at $p_{O_2} = 100$ Pa. The experimental conditions were selected to match RABiTS and IBAD processing conditions. Phase diagrams of the $BaO–Tm_2O_3–CuO_z$ [22,23] and $BaO–Yb_2O_3–CuO_z$ [24,25] systems are available in literature; however, partly because it is difficult to handle BaO, the majority of these diagrams were prepared using $BaCO_3$ as one of the starting reagents. The goal of the present paper is to report our studies of the R = Tm and R = Yb systems under conditions similar to our previous studies, i.e., $p_{O_2} = 100$ Pa, T = 750 °C and 810 °C, with BaO as a source

* Corresponding author. Tel.: +1 301 975 5791; fax: +1 301 975 5334.
E-mail address: winnie.wong-ng@nist.gov (W. Wong-Ng).

0925-8388/$ – see front matter. Published by Elsevier B.V.
doi:10.1016/j.jallcom.2006.07.083

Table 1
Samples prepared for the phase relationship studies in the BaO–Tm_2O_3–CuO_z and BaO–Yb_2O_3–CuO_z systems at p_{O_2} = 100 Pa, and T = 750 °C and 810 °C

No.	Ba	Tm/Yb	Cu	No.	Ba	Tm/Yb	Cu
1	60	10	30	2	50	17	33
3	65	17.5	17.5	4	70	5	25
5	58	3	39	6	42.86	57.14	0
7	54	8	38	7	45	15	40
9	40	40	20	9	60	35	5
11	40	20	40	12	35	60	5
13	20	70	10	14	25	25	50
15	40	5	55	16	25	5	70
17	10	35	55	18	10	65	25
19	50	25	25	20	45	10	45
21	35	53	12	22	50	40	10
23	35	20	45	24	33.33	16.67	50
25	32	18	50	26	63	3	34
27	50	12.5	37.5	28	33.33	66.67	0

In the table, Ba stands for BaO, Tm/Yb stands for 1/2(Tm_2O_3) or 1/2(Yb_2O_3), and Cu stands for CuO. The numbers in the table correspond to mole fraction, %.

for Ba. The crystal chemistry and crystal structure of compounds of the BaO–R_2O_3–CuO_z systems have been reported extensively in literature and will not be discussed in detail here. Emphasis will be placed on the phase formation and phase compatibilities, which are important for coated conductor processing.

2. Experimental details[1]

2.1. Preparation of BaO

BaO starting material was produced from $BaCO_3$ (99.99% purity, metals basis) by vacuum calcination in a custom-designed vertical tube furnace. An MgO crucible containing ~15 g of $BaCO_3$ was suspended in the hot zone of the furnace, and the furnace was evacuated to a pressure of ~10 μmHg or less by a high capacity mechanical pump. The temperature of the sample was raised from room temperature to 1300 °C in 20 h, followed by an isothermal heat-treatment at 1300 °C for 10 h, and then cooled from 1300 °C to room temperature in 20 h. During vacuum calcination the pressure typically increased to ~200 μmHg as CO_2 was evolved, and then rapidly returned to ~10 μmHg or less as the decomposition of the $BaCO_3$ was completed. After cooling, the BaO was lowered through an interlock into a transfer vessel. It was then transported to an Ar-filled glove-box continually purged with a recirculating purifier, which removed atmospheric contaminants from the Ar to <1 ppm by volume. Characterization by X-ray powder diffraction showed only the characteristic peaks for BaO.

2.2. Sample preparation

All sample weighings, homogenizations and pressings of pellets were performed inside the glove-box to avoid contamination with CO_2 and H_2O. Pelletized samples were placed inside individual MgO crucibles for annealing in a horizontal box-type controlled-atmosphere furnace. Transfer from the glove-box to the box furnace and vice versa was achieved via a second transfer vessel and an interlock system attached to the furnace.

The solid-state sintering method was used to prepare 28 samples each for the BaO–Tm_2O_3–CuO_z system and for the BaO–Yb_2O_3–CuO_z system (Table 1). Stoichiometric amounts of BaO, R_2O_3 (R = Tm and Yb) (99.99% purity, metals basis), and CuO (99.99% purity, metals basis) were mixed and pressed into pellets, and annealed in the box furnace. During the annealings, the oxygen pressure of Ar/O_2 mixtures was controlled using a mass flow meter and monitored at both the inlet and outlet of the furnace using a zirconia oxygen sensor. Samples were annealed at 750 °C and at 810 °C for the experiments at p_{O_2} = 100 Pa (0.1% O_2 by volume). Intermediate grindings and pelletizings took place until no further changes were detected in the powder X-ray diffraction patterns. Samples were processed for about 3 weeks each.

2.3. X-ray powder diffraction

For X-ray phase analysis, specimens were loaded into a hermetic cell designed for air-sensitive materials [26]. The process of sample loading was performed inside an Ar-filled glove-box. X-ray powder diffraction was used to identify the phases synthesized and to confirm phase purity. Data were collected using a computer-controlled automated diffractometer equipped with a theta-compensation slit; Cu Kα radiation was used at 45 kV and 40 mA. The radiation was detected by a scintillation counter and a solid-state amplifier. A Siemens diffraction software package and reference X-ray diffraction patterns of the ICDD Powder Diffraction File (PDF) [27] were used for phase identification.

3. Results and discussion

Figs. 1–4 give the phase diagrams of the BaO–Tm_2O_3–CuO_z and the BaO–Yb_2O_3–CuO_z systems. These diagrams appear to be relatively simple, but are different from those prepared using $BaCO_3$ [22–25], particularly in the Ba-rich region. Due to the substantially different ionic size of Tm^{3+} and Ba^{2+} (0.994 Å versus 1.42 Å), and Yb^{3+} and Ba^{2+} (0.985 Å versus 1.42 Å) [28], respectively, there is no detectable solid solution formation of compounds in these systems under the current experimental conditions.

3.1. Phase formation

3.1.1. BaO–Tm_2O_3–CuO_z system

3.1.1.1. The BaO–CuO_z System. A review of the crystal chemistry and crystallography of the phases in the BaO–CuO_z system was given by Wong-Ng and Cook [29], and therefore the details

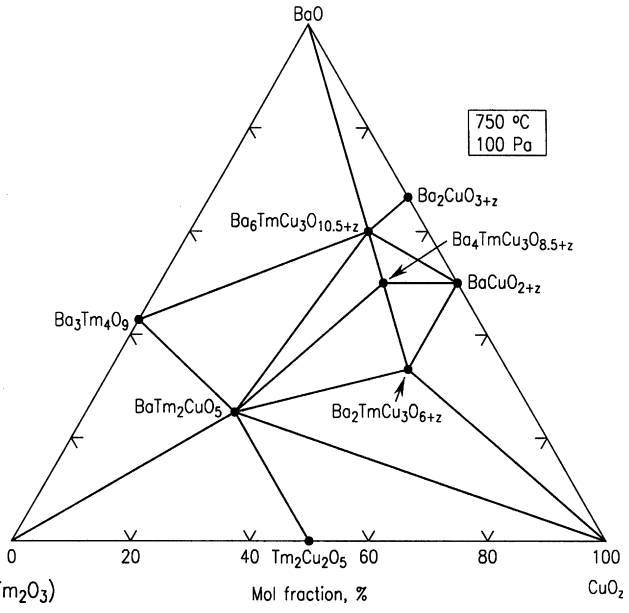

Fig. 1. Phase diagram of the BaO–1/2Tm_2O_3–CuO_z system prepared at p_{O_2} = 100 Pa and ≈750 °C, using BaO starting material.

[1] Certain commercial equipment, instruments, or materials are identified in this paper to foster understanding. Such identification does not imply recommendation or endorsement by the National Institute of Standards and Technology, nor does it imply that the materials or equipment identified are necessarily the best available for the purpose.

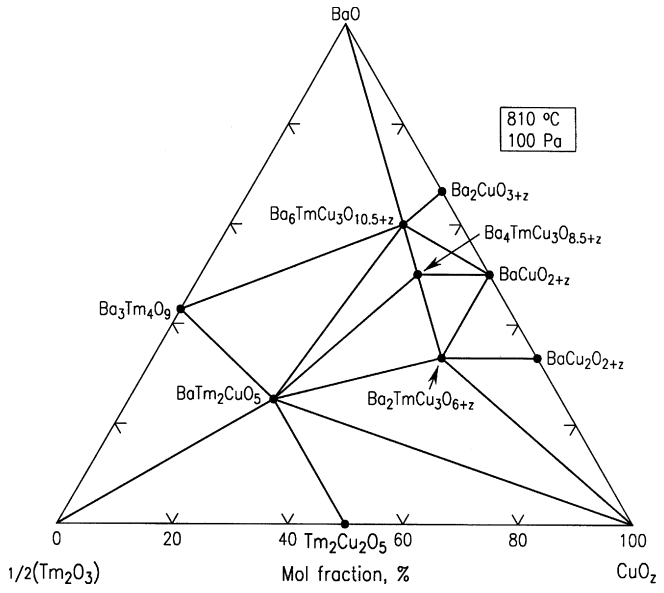

Fig. 2. Phase diagram of the BaO–1/2Tm_2O_3–CuO_z system prepared at p_{O_2} = 100 Pa and ≈810 °C, using BaO starting material.

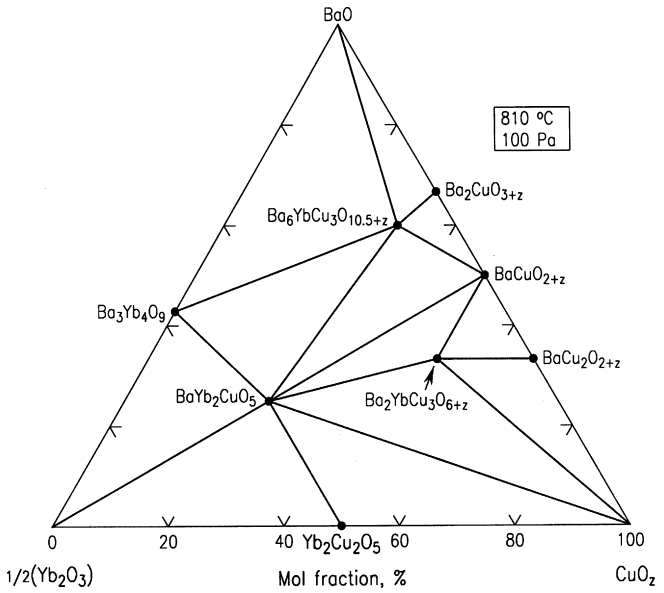

Fig. 4. Phase diagram of the BaO–1/2Yb_2O_3–CuO_z system prepared at p_{O_2} = 100 Pa and ≈810 °C, using BaO starting material.

will not be discussed here. At both 750 °C and 810 °C, the compounds Ba_2CuO_{3+z} and $BaCuO_{2+z}$ were found to be stable at p_{O_2} = 100 Pa [29–34]. The Ba_2CuO_{3+z} phase is atmospherically sensitive, and cannot be prepared in the presence of moisture and carbonate. The oxygen content of the $BaCuO_{2+z}$ series has been reported to vary between 2.0 and 2.5 [29]. Three structure types are known ($0 < z < 0.12$, $0.29 < z < 0.36$, and $z = 0.5$). The most commonly recognized structure form is cubic, with $0 < z < 0.12$. Phase compositions with z greater than 0.12 have been reported by Petricek et al. [34]. At 810 °C, we found that the reduced phase $BaCu_2O_{2+z}$ was observed in addition to Ba_2CuO_{3+z} and $BaCuO_{2+z}$. Also, CuO was found to be reduced to Cu_2O. There is no evidence for the existence of the $Ba_2Cu_3O_{5+z}$ or $Ba_3Cu_5O_{8+z}$

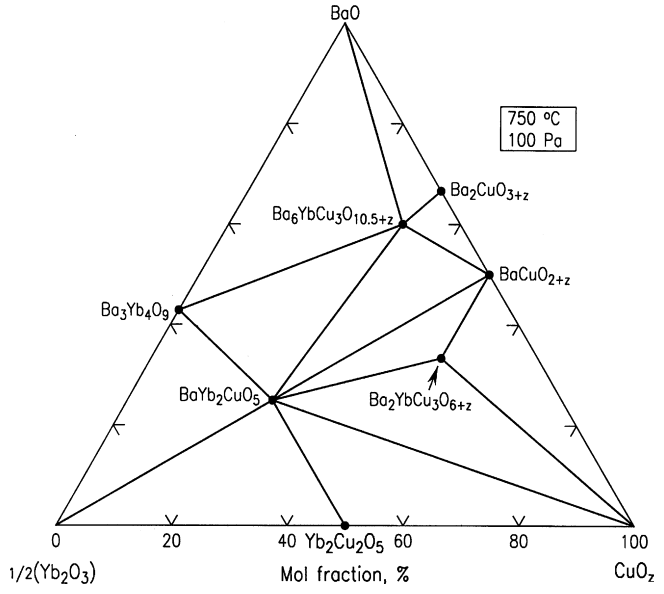

Fig. 3. Phase diagram of the BaO–1/2Yb_2O_3–CuO_z system prepared at p_{O_2} = 100 Pa and ≈750 °C, using BaO starting material.

phases [30]. The Ba_3CuO_4 phase, reported by Frase and Clarke [35] and Abbattista et al. [36,37] to be stable under very reduced conditions, was not detected in the present study. In contrast to the BaO–Nd_2O_3–CuO_z [17], BaO–Sm_2O_3–CuO_z [18], and the BaO–Eu_2O_3–CuO_z [21] systems where one observes the formation of the (Ba, R)$_2CuO_{3+z}$ phase, no solid solution formation of the (Ba, Tm)$_2CuO_{3+z}$ system was found due to the large difference in the ionic size of Ba and Tm [28].

3.1.1.2. BaO–Tm_2O_3. Different from the BaO–Y_2O_3 [19] and BaO–Er_2O_3 [20] systems, the $Ba_3R_4O_9$ but not BaR_2O_4 phase was found to be stable in the BaO–Tm_2O_3 system at both 750 °C and 810 °C. The $Ba_2R_2O_5$ and $Ba_4R_2O_9$-type phases as reported in the BaO–Y_2O_3–CuO_z system (prepared with $BaCO_3$-derived starting materials [38]) are not stable here. The Y-analogs of these phases have been determined by Abbattista et al. [37] and DeLeeuw et al. [32] to correspond to $Ba_2Y_2O_5{\cdot}CO_2$ and $Ba_4Y_2O_9{\cdot}2CO_2$.

3.1.1.3. Tm_2O_3–CuO_z. At both 750 °C and 810 °C, only the $Tm_2Cu_2O_5$ phase was observed in the Tm_2O_3–CuO_z diagram [39]. The R_2CuO_4 type phase only exists when R is relatively large ($r_{R^{3+}} > r_{Dy^{3+}}$). As $r_{R^{3+}}$ decreases beyond Gd (namely, from Dy to Lu), the $R_2Cu_2O_5$ type phase (orthorhombic, $Pna2_1$) was found instead of R_2CuO_4 [13]. Furthermore, the reported reduced phase of the $YCuO_2$ structure type [40,41] was not found; presumably the oxygen partial pressure of p_{O_2} = 100 Pa is not sufficiently low to stabilize this phase.

3.1.1.4. BaO–Tm_2O_3–CuO_z. At both 750 °C and 810 °C, a total of four ternary oxides ($Ba_2TmCu_3O_{6+z}$, $Ba_4TmCu_3O_{8.5+z}$, $Ba_6TmCu_3O_{10.5+z}$, and the 'green phase' $BaTm_2CuO_5$) were found in the BaO–Tm_2O_3–CuO_z system (Figs. 1 and 2). The formation of the compounds $Ba_4RCu_3O_{8.5+z}$ and $Ba_6RCu_3O_{10.5+z}$ in the BaO-rich part of the diagram is similar to that in the

$BaO–Y_2O_3–CuO_z$, $BaO–Ho_2O_3–CuO_z$ and $BaO–Er_2O_3–CuO_z$ systems [19–21,24]. The structure of $Ba_4TmCu_3O_{8.5+z}$ was reported to be of the cubic oxygen-defect perovskite type ($a = 8.07670(8)$ Å when prepared in oxygen) [42,43]. The orthorhombic $Ba_6TmCu_3O_{10.5+z}$ phase is of the $SrTi_2O_4$-type (layered perovskite structure) [44]. The structure of the $BaTm_2CuO_5$ "green" phase (orthorhombic with space group *Pnma*), has been studied extensively [13,45–47]. This phase, however, has a different structure from that of the Nd-brown phase ($BaNd_2CuO_5$) [17].

Similar to the $Ba_2RCu_3O_{6+z}$ analogs (R = Y, Er, Ho), $Ba_2TmCu_3O_{6+z}$ is a stoichiometric compound with respect to the cation content. By contrast, solid solution formation was reported in the lanthanide-containing $Ba_{2-x}R_{1+x}Cu_3O_{6+z}$ phases with relatively larger size of R (for example, $R = Nd^{3+}$ (1.109 Å), Sm^{3+} (1.079 Å), and Eu^{3+} (1.004 Å)) [28] when samples were also prepared under 100 Pa [17,18,21].

3.1.2. $BaO–Yb_2O_3–CuO_z$ system

The phases determined in the $BaO–CuO_z$ system, namely, Ba_2CuO_{3+z}, $BaCuO_{2+z}$ (under both 750 °C and 810 °C), and an additional $BaCu_2O_{2+z}$ phase while the diagram was prepared under 810 °C have already been discussed above.

3.1.2.1. $BaO–Yb_2O_3$. The binary diagram of the $BaO–Yb_2O_3$ system was reported by Lopato et al. [48]. Under both 750 °C and 810 °C (Figs. 3 and 4), the $Ba_3Yb_4O_9$ phase was the only compound found in the binary $BaO–Yb_2O_3$ system. $Ba_3Yb_4O_9$ was reported to crystallize in the rhombohedral $R\bar{3}m$ system [49], which is isostructural with the $Ba_3Tm_4O_9$ and $Ba_3Y_4O_9$ structure [19]. The BaR_2O_4 type phase (orthorhombic *Pnam*) which exists in systems with larger R^{3+} (for example, R = Ho, Y, Er, etc.) [50] cannot be prepared with the relatively small Yb^{3+}. Similar to the Tm-analog, the $Ba_4R_2O_7$ and $Ba_2R_2O_5$ phases which were reported when $BaCO_3$ was used as a starting reagent, were found to be absent under carbonate-free conditions.

3.1.2.2. $Yb_2O_3–CuO_z$. The phase diagram of the $Yb_2O_3–CuO_z$ system prepared in air was reported by Chen et al. [51]. Similar to the Tm-analog, only the $Yb_2Cu_2O_5$ phase was obtained under 750 °C and 810 °C. Neither the Yb_2CuO_4 type phase nor the rhombohedral $YbCuO_2$ ($RCuO_2$ structure type [40,41]) was found.

3.1.2.3. $BaO–Yb_2O_3–CuO_z$. There are a total of three ternary oxide phases in the $BaO–Yb_2O_3–CuO_z$ system, namely, $Ba_2YbCu_3O_{6+z}$, $BaYb_2CuO_5$, and $Ba_6YbCu_3O_{10.5+z}$. Due to the great mismatch of the size of Yb^{3+} and Ba^{2+} (0.985 Å versus 1.42 Å) [28], solid solution formation was not found in this system. Our results agree with those of Osamura and Zhang [24] in that in the temperature range of 750–810 °C, the $Ba_2YbCu_3O_{6+z}$ phase is stable at oxygen partial pressures below approximately 10^4 Pa. At higher temperatures, a mixture of $BaYb_2CuO_5$, $BaCuO_{2+z}$, and CuO was obtained instead. The $Ba_6YbCu_3O_{10.5+z}$ phase was reported by Zhang and Osamura to be perovskite-related [44]. Similar to the $Ba_6ErCu_3O_{10.5+z}$, $Ba_6YCu_3O_{10.5+z}$, and $Ba_6HoCu_3O_{10.5+z}$ phases [19], $Ba_6YbCu_3O_{10.5+z}$ was reported to be orthorhombic (*Immm*, $a = 3.9830(2)$ Å, $b = 4.0986(2)$ Å, and $c = 21.571(1)$ Å) when prepared in air [44]. While the $Ba_4YbCu_3O_{8.5+z}$ phase can be prepared at $p_{O_2} = 0.1$ MPa or $p_{O_2} = 0.022$ MPa (air) [44,52], it cannot be prepared at $p_{O_2} = 100$ Pa. The 'green phase' $BaYb_2CuO_5$ is isostructural to $BaTm_2CuO_5$ [13].

3.2. Phase Compatibilities

3.2.1. $BaO–Tm_2O_3–CuO_z$

The tie-lines determined near the CuO_z and Tm_2O_3 regions are in agreement with those determined in most other $BaO–R_2O_3–CuO_z$ diagrams, whether prepared using $BaCO_3$, BaO_2, BaO, or $Ba(NO_3)_2$. However, the BaO-rich regions of the diagrams are substantially different from each other. This diagram of the Tm-system prepared using BaO is somewhat different to that of the $BaO–Y_2O_3–CuO_z$ system reported by us [19]. The tie-line relationships around the 213 phase which involve the four phases, $Ba_2TmCu_3O_{6+z}$, $BaTm_2CuO_5$, $BaCuO_{2+z}$, and $Ba_4TmCu_3O_z$ are also different from the literature data. For example, in the present study, the $Ba_2TmCu_3O_{6+z}$ phase is found to be compatible to the $Ba_4TmCu_3O_z$ phase, whereas most literature phase diagrams of the $BaO–R_2O_3–CuO_z$ systems involve a tie-line between $BaCuO_{2+z}$ and BaR_2CuO_5 [13,19,22,23,53–58]. The $Ba_2RCu_3O_{6+z}$–$Ba_4RCu_3O_z$ tie-line was also found in our previous studies of the Nd-, Sm-, Eu, Dy-, Ho-, Y-, and Er-systems [17–21], and during the investigation of the melting equilibria of the $BaO–Y_2O_3–CuO_z$ system [59]. The majority of literature studies were not conducted entirely under atmospherically-controlled conditions, and it is clear that the presence of CO_2 affects the tie-line relationships.

3.2.2. $BaO–Yb_2O_3–CuO_z$

The tie-line distribution in the Ba-poor region of the $BaO–Yb_2O_3–CuO_z$ system, as shown in Figs. 3 and 4, is in general similar to that found in the $BaO–Tm_2O_3–CuO_z$ system. Unexpectedly, we found that at both 750 °C and 810 °C, there is a tie-line connecting the $BaCuO_{2+z}$ phase to the 'green phase', $BaYb_2CuO_5$. This is different from other $BaO–R_2O_3–CuO_z$ systems while the size of R^{3+} is larger than that of Yb^{3+}. Therefore, whether a tie-line exists between BaR_2CuO_5 and $BaCuO_{2+z}$, or between $Ba_2RCu_3O_{6+z}$ and a barium-rich phase appears to depend on the condition of preparation and the size of R^{3+}. A comparison of the $BaO–Yb_2O_3–CuO_z$ diagrams (Figs. 1 and 2) to the $BaO–Tm_2O_3–CuO_z$ diagrams (Figs. 3 and 4) indicates that the absence of the $Ba_4YbCu_3O_{8.5+z}$ phase affects the tie-line relations in the region bounded by $BaCuO_2$, $Ba_2YbCu_3O_{6+z}$, $BaYb_2CuO_5$, and $Ba_6YbCu_3O_{10.5+z}$. All ternary oxides are compatible with at least four other phases. In the case of $BaYb_2CuO_5$, seven tie-lines were found to originate from it. In the BaO-rich region, tie-lines are found between BaO and $Ba_6YbCu_3O_z$.

3.2.3. Implications for processing

For applications of phase equilibria to coated conductor processing, phase diagrams constructed under carbonate-free conditions should be employed. An examination of Figs. 1–4

shows a significant difference in the tie-line distributions occurring under carbonate-free conditions, relative to those occurring in the phase diagrams based on $BaCO_3$-derived starting materials [22–25]. Under carbonate-free conditions at a p_{O_2} of 100 Pa, the $Ba_2TmCu_3O_{6+z}$–$Ba_4TmCu_3O_z$ tie-line replaces a $BaCuO_{2+z}$–$BaTm_2CuO_5$ tie-line in the $BaO–Tm_2O_3–CuO_z$ system; and a $BaCuO_{2+z}$–$BaYb_2CuO_5$ tie-line replaces the $Ba_2YbCu_3O_{6+z}$–$Ba_6YbCu_3O_z$ tie-line in the $BaO–Yb_2O_3–CuO_z$ system. The net effect of this difference is that in the Tm-case, there is an expansion of the field of stability of Tm-213 towards the BaO-rich corner of the phase diagram as compared to the Yb-213 phase; $Ba_4TmCu_3O_{8.5+z}$ can coexist with Tm-213. However, because $Ba_4RCu_3O_{8.5+z}$ is atmospherically more sensitive than BaR_2CuO_5, its presence in R-213 materials could be deleterious. It may be important during the RABiTS and IBAD processes to avoid bulk compositions in this region.

4. Summary

We have investigated the phase relationships of the $BaO–Tm_2O_3–CuO_z$ and the $BaO–Yb_2O_3–CuO_z$ systems at p_{O_2} = 100 Pa under both 750 °C and 810 °C. Sample preparation and handling were accomplished using a glove-box filled with argon and an atmospherically-controlled furnace and apparatus. Similar to the Nd-, Sm-, Eu-, Gd-, Dy-, Ho-, Y-, and Er-systems that we have reported previously [17–21], the presence of CO_2 affects the tie-line relationships. For example, the tie-line relationships among the four phases, $BaTm_2CuO_5$, $Ba_2TmCu_3O_z$, $BaCuO_{2+z}$, and $Ba_4TmCu_3O_{8.5+z}$ are different from the literature data. A tie-line between $Ba_2TmCu_3O_z$ and $Ba_4TmCu_3O_{8.5+z}$ was observed. In the Yb-system, a tie-line between $BaYb_2CuO_5$ and $BaCuO_{2+z}$ was found instead. It appears that whether a tie-line exists between BaR_2CuO_5 and $BaCuO_{2+z}$, or between $Ba_2RCu_3O_{6+z}$ and a barium-rich phase appears to depend on the condition of preparation and the size of R^{3+}. In addition, due to the absence of the $Ba_4YbCu_3O_{8.5+z}$ phase in the Yb-analog, the tie-line relations are different in the $BaO–Yb_2O_3–CuO_z$ and the $BaO–Tm_2O_3–CuO_z$ systems.

Phase diagrams of the $BaO–R_2O_3–CuO_z$ (R = lanthanides) systems are important for coated-conductor development, and it is anticipated that systematic studies of diagrams of these systems under relevant atmospherically-controlled conditions will continue.

Acknowledgements

The US Department of Energy is acknowledged for partial financial support of this project. The authors would like to express thanks to Mr. N. Swanson and Dr. P. Schenck for their assistance with the phase diagram graphics.

References

[1] J.G. Bednorz, K.A. Müller, Z. Phys. B 64 (1986) 189.
[2] U. Balachandran, A.N. Iyer, P. Haldar, J.G. Hoehn, L.R. Motowidlo, in: K. Krishen, C. Burnham (Eds.), Proceedings of The Fourth International Conference and Exhibition: World Congress on Superconductivity, Orlando, FL, June 27–July 1, vol. II, 1994, p. 639.
[3] W.G. Wang, Z. Han, P. Skov-Hansen, J. Goul, M.D. Bentzon, P. Vase, Y.L. Lin, IEEE Trans. Appl. Supercond. 9 (1999) 2613.
[4] R. Zeng, B. Ye, J. Horvat, Y.C. Guo, B. Zeimetz, X.F. Yang, T.P. Beales, H.K. Liu, S.X. Dou, Supercond. Sci. Technol. 11 (1998) 1101.
[5] R.M. Baurceanu, V.A. Maroni, N.M. Merchant, A.K. Fischer, M.J. McNallan, R.D. Parrella, Supercond. Sci. Technol. 15 (2002) 1167.
[6] A.P. Malozemoff, W. Carter, S. Flexhler, L. Fritzemeier, Q. Li, L. Masur, D. Parker, R. Parrella, E. Pedtburg, G.N. Riley, M. Rupich, J. Scudiere, W. Zhang, IEEE Trans. Appl. Supercond. 9 (1999) 2469.
[7] A.P. Malozemoff, S. Annavarapu, L. Fritzemeier, Q. Li, V. Prunier, M. Rupich, C. Thieme, W. Zhang, A. Goyal, M. Paranthaman, D.F. Lee, Supercond. Sci. Technol. 13 (2000), 473-376.
[8] A. Goyal, D.F. Lee, F.A. List, E.D. Specht, R. Feenstra, M. Paranthaman, X. Cui, S.W. Lu, P.M. Martin, D.M. Kroeger, D.K. Christen, B.W. Kang, D.P. Norton, C. Park, D.T. Verebelyi, J.R. Thompson, R.K. Williams, T. Aytug, C. Cantoni, Physica C 357 (2001) 903.
[9] T. Aytug, A. Goyal, N. Rutter, M. Paranthaman, J.R. Thompson, H.Y. Zhai, D.K. Christen, J. Mater. Res. 18 (4) (2003) 872.
[10] S.R. Foltyn, E.J. Peterson, J.Y. Coulter, P.N. Arendt, Q.X. Jia, P.C. Dowden, M.P. Maley, X.D. Wu, D.E. Peterson, J. Mater. Res. 12 (1997) 2941.
[11] M. Bauer, R. Semerad, H. Kinder, IEEE Trans. Appl. Supercond. 9 (2) (1999) 1502.
[12] J.L. MacManus-Driscoll, Advanced Materials 9 (6) (1997) 457–473.
[13] W. Wong-Ng, B. Paretzkin, E.R. Fuller Jr., J. Solid State Chem. 85 (1) (1990) 117.
[14] T.B. Lindemer, F.A. Washburn, C.S. MacDougall, O.B. Cavin, Physica C 174 (1991) 135–143.
[15] Y. Le Page, T. Siegrist, S.A. Sunshine, L.F. Schneemeyer, D.W. Murphy, S.M. Zahurak, J.V. Waszczak, W.R. McKinnon, J.M. Tarascon, G.W. Hull, L.H. Greence, Phys. Rev. B 36 (1987) 3617.
[16] Partnership for Superconducting Technology, Office of Power Technology, Office of Energy Efficiency and Renewable Energy, US Department of Energy.
[17] W. Wong-Ng, L.P. Cook, J. Suh, R. Coutts, J.K. Stalick, I. Levin, Q. Huang, J. Solid State Chem. 173 (2003) 476.
[18] W. Wong-Ng, L.P. Cook, J. Suh, J.A. Kaduk, Physica C 405 (2004) 47–58.
[19] W. Wong-Ng, L.P. Cook, J. Suh, Physica C 377 (2002) 107–113.
[20] W. Wong-Ng, L.P. Cook, J. Suh, Solid State Sci. 6 (11) (2004) 1211–1216.
[21] W. Wong-Ng, Z. Yang, L.P. Cook, J. Frank, M. Loung, Physica C 439 (2006) 93–100.
[22] S.N. Koshcheeva, V.A. Fotiev, A.A. Fotiev, V.G. Zubkov, Izv. Akad. Nauk SSSR, Neorg. Mater. 26 (7) (1990) 1491–1494;
S.N. Koshcheeva, V.A. Fotiev, A.A. Fotiev, V.G. Zubkov, Inorg. Mater. 26 (7) (1990) 1267–1270.
[23] E. Hodorowicz, S.A. Hodorowicz, H.A. Eick, Physica C 158 (1–2) (1989) 127–136.
[24] K. Osamura, W. Zhang, Z. Metallkd. 84 (8) (1993) 522–528.
[25] J.K. Liang, X.L. Chen, S. Wu, J. Zhao, Y.L. Zhang, S. Xie, Solid State Commun. 74 (6) (1990) 509–516.
[26] J.J. Ritter, Powder Diffr. 3 (1) (1988) 30.
[27] Powder Diffraction File (PDF), Produced by International Centre for Diffraction Data (ICDD), 12 Campus Blvd., Newtown Square, PA 19073-3273.
[28] R.D. Shannon, Acta Crystallogr. A32 (1976) 751.
[29] W. Wong-Ng, L.P. Cook, Powder Diffr. 9 (4) (1994) 280.
[30] W. Wong-Ng, K. Davis, R.S. Roth, J. Am. Ceram. Soc. 71 (2) (1988) C64.
[31] J.L. Luce, A.M. Stacy, Chem. Mater. 9 (1997) 1508.
[32] D.W. Deleeuw, H.A. Mutsaers, C. Langereis, H.C.A. Smoorenburg, P.J. Rommers, Physica C 152 (1988) 39.
[33] J. Thompson, J.D. FitzGerald, R.L. Withers, P.J. Barlov, J.S. Anderson, Mater. Res. Bull. 24 (1989) 505.
[34] S. Petricek, N. Bukovec, P. Bukovec, J. Solid State Chem. 99 (1992) 58.
[35] K.G. Frase, D.R. Clarke, Adv. Ceram. Mater. 2 (3B) (1987) 295.
[36] F. Abbattista, M. Vallino, D. Mazza, Chem. Phys. 21 (1989) 521.
[37] F. Abbattista, M. Vallino, D. Mazza, M.L. Borlera, C. Brisi, Mater. Chem. Phys. 20 (2) (1988) 191.

[38] R.S. Roth, C.J. Rawn, F. Beech, J.D. Whitler, J.O. Anderson, in: M.F. Yan (Ed.), Ceramic Superocnductors II, American Ceramic Society, Westerville, OH, 1988, pp. 13–26.
[39] H.R. Freund, H. Muller-Buschbaum, Z. Naturforsch Teil B 32 (1977) 609.
[40] T. Ishiguro, N. Ishizawa, N. Mizutani, M. Kato, J. Solid State Chem. 49 (1983) 232.
[41] B.U. Kohler, M. Jansen, Z. Anorg. Allg. Chem. 543 (1986) 73.
[42] Y. Zhu, Set 51-1678, Powder Diffraction File, Produced by ICDD, 12 Campus Blvd. Newtown Square, PA 19081, 2000.
[43] Y. Zhu, E.J. Peterson, P.S. Baldonado, J.Y. Coulter, D.E. Peterson, F.M. Maeller, J. Alloys Compd. 281 (1998) 137.
[44] W. Zhang, K. Osamura, Physica C 174 (1991) 135–143.
[45] R.M. Hazen, L.W. Finger, R.J. Angel, C.T. Prewitt, N.L. Ross, H.K. Mao, C.G. Hadidiacos, P.H. Hor, R.L. Meng, C.W. Chu, Phys. Rev. B 35 (1987) 7238.
[46] S.F. Watkins, F.R. Fronczek, K.S. Wheelock, R.G. Goodrich, W.O. Hamilton, W.W. Johnson, Acta Crystallogr. C44 (1988) 3–6.
[47] W. Wong-Ng, M.A. Kuchinski, H.F. McMurdie, B. Paretzkin, Powder Diffr. 4 (1989) 2–8.
[48] L.M. Lopato, I.M. Maister, A.V. Shevchenko, Izv. Akad. Nauk SSSR, Neorg. Mater. 8 (5) (1972) 861–864;
L.M. Lopato, I.M. Maister, A.V. Shevchenko, Inorg. Mater (Engl. Transl.) 8 (5) (1972) 749–751.
[49] W. Wong-Ng, B. Paretzkin, Set 39-1401, Powder Diffraction File, Produced by ICDD, 12 Campus Blvd., Newtown Square, PA 19081, 1991.
[50] E. Hodorowicz, S.H. Hodorowicz, H. Eick, J. Solid State Chem. 84 (1990) 401.
[51] X.L. Chen, Y.Y. Ji, J.K. Liang, X.R. Cheng, J. Li, S.S. Xie, J. Alloys Compd. 191 (2) (1993) 297–300.
[52] M. Vallino, D. Mazza, F. Abbattista, J. Less-Common Met. 170 (1991) 83.
[53] H. Ouchi, H.M. Ito, Mater. Sci. Monogr. 70 (1991) 489.
[54] R.X. Liang, T. Nakamura, Jpn. J. Appl. Phys. Part 2 27 (7) (1988) L1277.
[55] S.A. Hodorowicz, A. Lasocha, W. Lasocha, A. Chodorowicz, H.A. Eick, Acta Phys. Pol. A75 (3) (1989) 437–442.
[56] J.K. Liang, X.T. Xu, G.H. Rao, S.S. Xie, X.Y. Shao, Z.G. Duan, J. Phys. D: Appl. Phys. 20 (1987) 1324.
[57] S.A. Hodorowicz, A. Chodorowicz-Bak, J. Czerwonka, E. Hodorowicz, W. Lasocha, H.A. Eick, J. Solid State Chem. 92 (2) (1991) 480.
[58] Y.L. Zhang, J.K. Liang, X.R. Chen, G.H. Rao, H.B. Liu, Y.M. Ni, D.N. Zheng, S.S. Xie, J. Less-Common Met. 146 (1989) 121.
[59] W. Wong-Ng, L.P. Cook, J. Res. Natl. Inst. Stand. Technol. 103 (1998) 379–403.